

Synergistic Effect of Charge Separation and Defect Passivation Induced via Zinc Porphyrin Dye Incorporation for Efficient and Stable Perovskite Solar Cells

Yu Zhou, Han Zhong, Jianhua Han, Meiqian Tai, Xuewen Yin, Minghua Zhang, Ziyi Wu, Hong Lin*

Materials. Unless specified, all of the reagents and solutions were purchased from either Alfa Aesar or Sigma Aldrich. $\text{NH}_2\text{CHNH}_2\text{I}$ (FAI) and $\text{CH}_3\text{NH}_3\text{Br}$ (MABr) were purchased from Greatcell Solar. YD2-*o*-C8 was purchased from Everlight Chemical. Spiro-OMeTAD (99.7%) was bought from Borun Chemical Co., Ltd. All the materials were used as received without any purification.

Device fabrication. ITO-coated glasses were etched and cleaned in sequence with detergent, deionized water, ethanol, acetone and isopropanol. Before use, ITO glasses were blown to dry by N_2 and exposed to O_2 plasma for 15 min. SnO_2 precursor solution (2.5 wt% in H_2O) was prepared by diluting the SnO_2 colloidal dispersion (15 wt% in H_2O). The SnO_2 precursor solution was spin coated at 4000 rpm for 30 s. The substrate was then heated at 150 °C for 40 min and cooled down slowly to room temperature on a hot plate. The NiO layer was prepared by our previous work.¹ YD2-*o*-C8 solutions were prepared by dissolving YD2-*o*-C8 in chlorobenzene (CB) with different concentration. The mixed cation perovskite precursor solution was obtained by dissolving FAI (1 M), PbI_2 (1.1 M), MABr (0.2 M) and PbBr_2 (0.2 M) in anhydrous

DMF/DMSO mixture with the volume ratio of 4 : 1. Then 1.5 M stock solution of CsI in DMSO, was added into the perovskite precursor with the volume ratio of 5 : 95. The perovskite precursor solution was stirred overnight and filtered with a 0.22 μm PTFE-filter before use. The perovskite solution was spin coated on the substrate (2000 rpm for 10 s, 6000 rpm for 20 s) with quick drop of 100 μL CB containing YD2-*o*-C8 at 10 s before the end of second spinning process. The intermediate film was then annealed at 100 $^{\circ}\text{C}$ for 60 min. The spiro-OMeTAD solution was prepared by dissolving 72.3 mg spiro-OMeTAD, 28.8 μL 4-*tert*-butylpyridine (tBP) and 17.5 μL lithium bis(trifluoromethylsulfonyl)imide (Li-TFSI) solution (520 mg/mL in acetonitrile) in 1 mL CB. The spiro-OMeTAD solution was spin coated on the perovskite film at 4000 rpm for 30 s. Subsequently, the film was kept in a dry box overnight to get oxidized. Finally, a 70 nm thick gold electrode was deposited by thermal evaporation.

Characterizations. In order to characterize the morphology and thickness of perovskite films, field-emission scanning electron microscopy (FESEM, Zeiss LEO1530, Germany) and atomic force microscopy (AFM, Cypher, Asylum Research Oxford Instruments) were deployed. X-ray photoelectron spectra (XPS) were recorded by photoelectron spectrometer (ESCALAB 250Xi, Thermo Fisher Scientific Inc., USA) to analyze the element information. The photoelectron spectroscopy in the air (PESA) was performed with the AC-2 PESA instrument (AC-2, RKI INSTRUMENTS, Japan) combining an open counter with a UV source to position the valence band. Ultraviolet-visible (UV-vis) absorption spectra were recorded via a Lambda 950 spectrophotometer (PerkinElmer, USA) at room temperature. Fourier transform

infrared spectroscopy (FTIR) measurements were performed using the ATR mode on the infrared spectrometer (VERTEX 70V, Bruker, Germany). Steady-state PL measurements were carried out by exciting the sample with a monochromatic xenon lamp source with a central wavelength of 460 nm. Time-resolved PL measurements were performed via a time-correlated single-photon counting system using a pulsed laser beam (EPL405) with a wavelength and frequency of 405 nm and 10-20 MHz. Photocurrent density–voltage (J – V) characteristics were tested with a digital source meter (2400, Keithley Instruments, USA) at a scan speed of 100 mV/s under AM 1.5G illumination. The samples were illuminated by a solar simulator calibrated with a standard crystalline silicon solar cell (91192, Oriel, USA). The active area (0.06 cm²) of the devices was determined by a black metal aperture. The monochromatic incident photon-to-electron conversion efficiency (IPCE) measurement was carried out with a QEX10 system (PV measurements, USA) on DC mode. The intensity of incident monochromatic light was calibrated with a standard silicon solar cell (1H020, PV Measurements, USA). Electrochemical impedance spectroscopy (EIS) was characterized under the Zahner system (Zahner, Zahner-Electrik GmbH & Co.KG, Germany). EIS was recorded at a potential of 1.0 V with a modulation amplitude of 10 mV at frequencies ranging from 1 Hz to 1 MHz in the dark. X-ray diffraction (XRD) patterns were obtained by employing a D8 Advance Diffractometer (Bruker, Germany) with a Cu-K α 1 (1.5406 Å) radiation operating at 40 kV and 40 mA.

DFT calculation. The theoretical simulation was conducted with the Vienna Ab Initio Simulation Package² based on density functional theory. Projector augmented wave

(PAW) was adopted to construct potentials to describe pseudopotential³ while exchange-correlation function was described by generalized gradient approximation (GGA).⁴ A $50 \times 50 \times 50$ Å cell holding 230 atoms was employed to search the best configuration and corresponding charge density distribution of YD2-*o*-C8 molecules. The cutoff energy of the projector augmented plane-wave basis set was 500 eV and the Brillouin zone was sampled using a single (Gamma) k-point. Hellman–Feynman force convergence was achieved at 0.03 eV/Å for full relaxation.

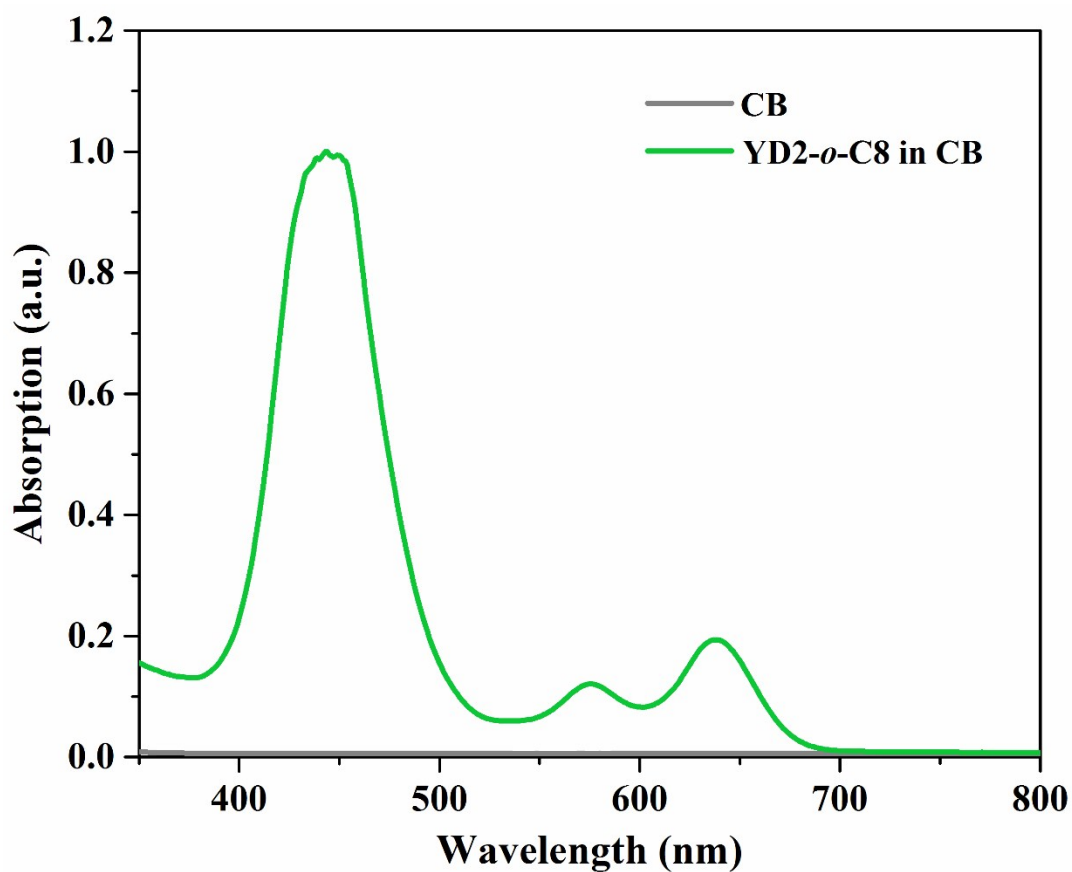


Figure S1. UV-vis absorption spectra of pristine chlorobenzene and YD2-*o*-C8 dissolved in chlorobenzene.

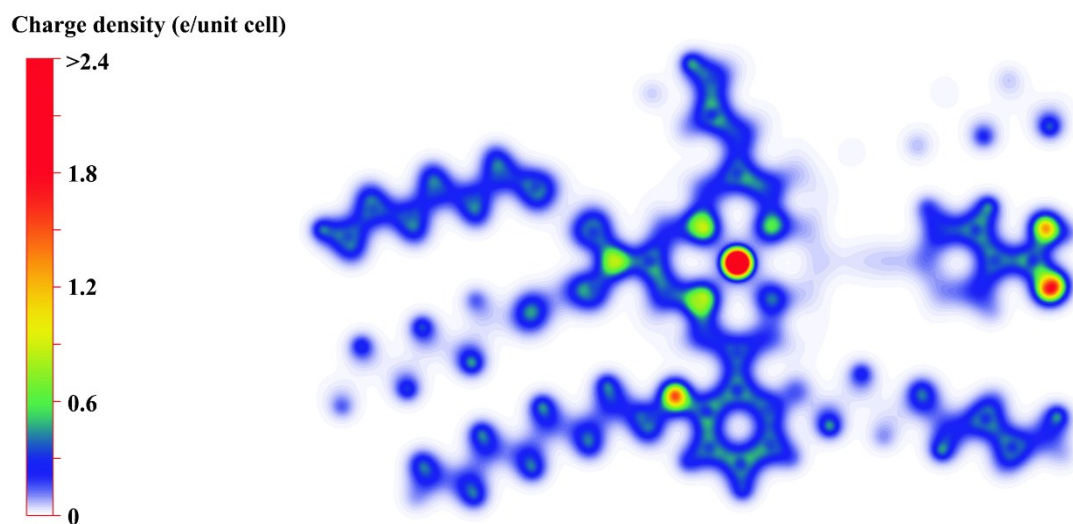


Figure S2. Calculated charge density distribution of YD2-*o*-C8 molecule.

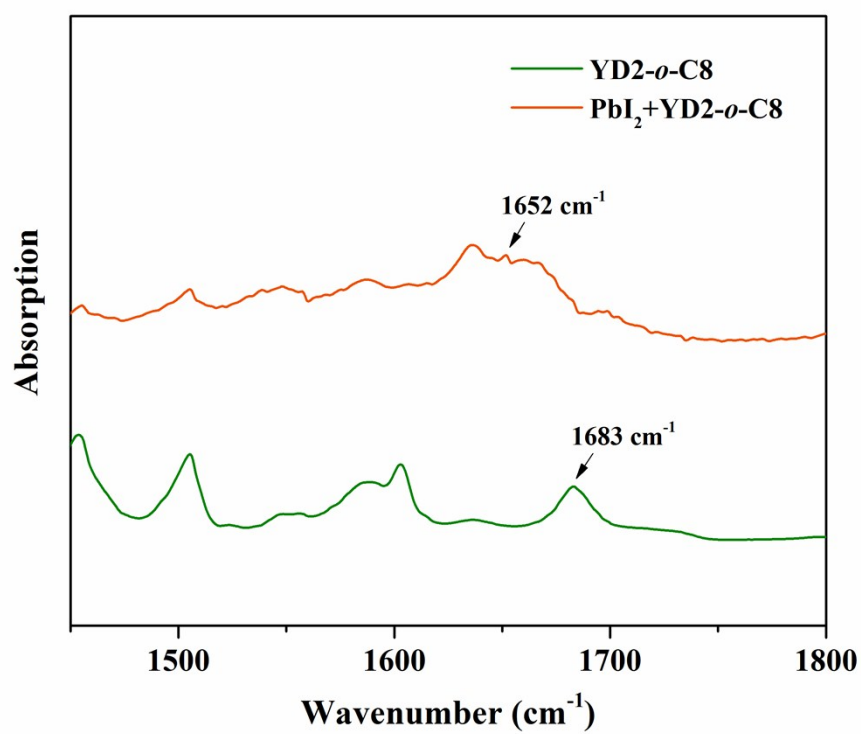


Figure S3. FTIR spectra of YD2-*o*-C8 and PbI₂ with YD2-*o*-C8.

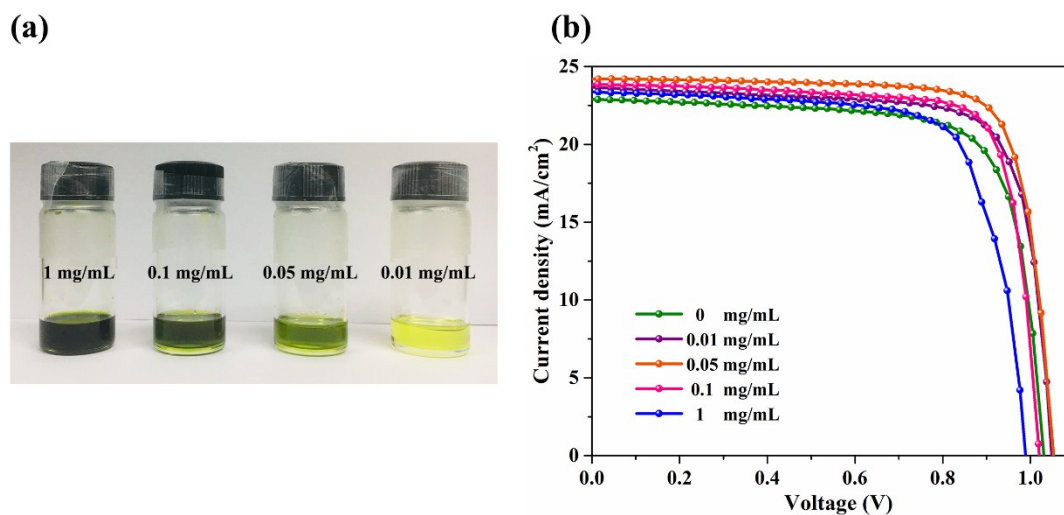


Figure S4. a) Physical photograph of chlorobenzene solutions with different YD2-*o*-C8 concentration. b) J - V curves of the corresponding PSCs modified with different YD2-*o*-C8 concentration.

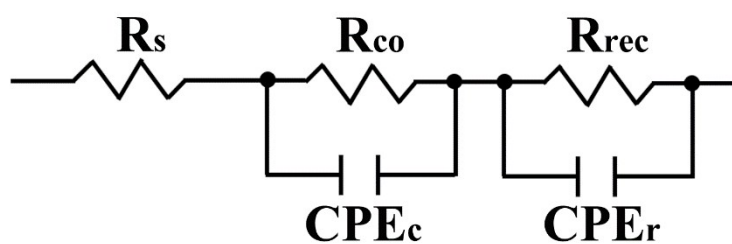


Figure S5. The equivalent circuit model of PSCs for EIS under dark condition.

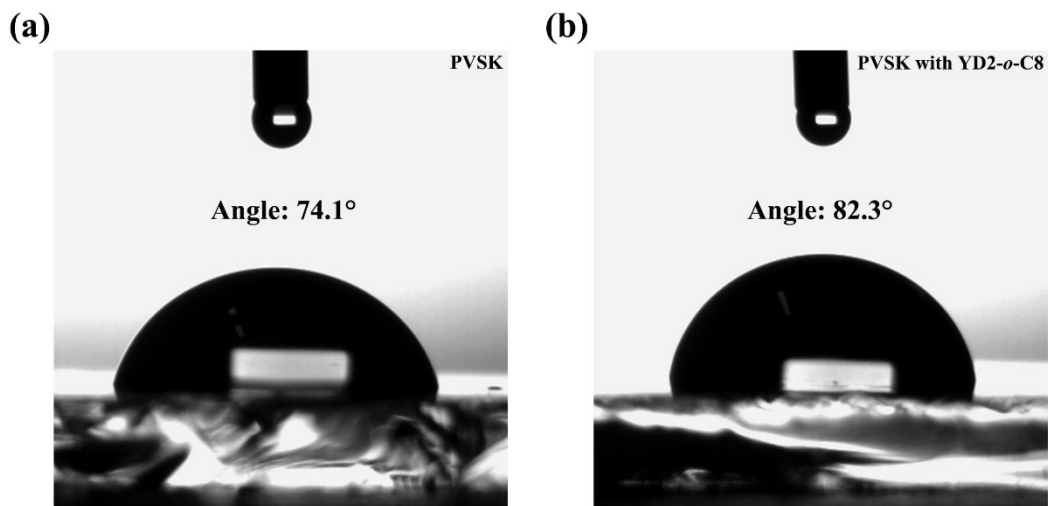


Figure S6. Contact angle tests with water on the surface of the corresponding PVSK films: a) control PVSK, b) YD2-*o*-C8 modified PVSK.

Table S1. Summary of fitted time-resolved photoluminescence spectra of C-PVSK and Y-PVSK on glass substrates.

Samples	A_1	τ_1 (ns)	A_2	τ_2 (ns)	τ_{avg}^* (ns)
C-PVSK	0.35	2.9	0.65	466.5	465.0
Y-PVSK	0.31	2.0	0.69	318.8	317.9

* τ_{avg} represents the average PL decay time fitted by the equation

$$\tau_{avg} = \frac{\sum A_i \tau_i^2}{\sum A_i \tau_i}$$

Table S2. Photovoltaic parameters derived from $J-V$ of PSCs based on Y-PVSK treated with different YD2-*o*-C8 concentrations from the same batch.

Concentration	J_{sc} (mA/cm ²)	V_{oc} (V)	FF	PCE (%)
0 mg/mL	22.9	1.03	0.75	17.7
0.01 mg/mL	23.7	1.04	0.77	19.0
0.05 mg/mL	24.2	1.05	0.79	20.1
0.1 mg/mL	23.8	1.02	0.78	18.9
1 mg/mL	23.4	0.99	0.73	16.9

Table S3. EIS parameters for PSCs under dark condition.

Perovskites	R_s (Ω)	R_{rec} (Ω)
C-PVSK	14.8	734.7
Y-PVSK	15.4	1136.0

1. X. Yin, J. Han, Y. Zhou, Y. Gu, M. Tai, H. Nan, Y. Zhou, J. Li and H. Lin, *J. Mater. Chem. A*, 2019, **7**, 5666-5676.
2. G. Kresse and J. Furthmüller, *Phys. Rev. B*, 1996, **54**, 11169-11186.
3. P. E. Blöchl, *Phys. Rev. B*, 1994, **50**, 17953-17979.
4. J. P. Perdew, K. Burke and M. Ernzerhof, *Phys. Rev. Lett.*, 1996, **77**, 3865-3868.